Gas bubble removal from a zero-gap alkaline electrolyser with a pressure swing and why foam electrodes might not be suitable at high current densities

Bleeker, Jorrit; van Kasteren, Celine; van Ommen, J. Ruud; Vermaas, David A.

DOI
10.1016/j.ijhydene.2024.01.147

Publication date
2024

Document Version
Final published version

Published in
International Journal of Hydrogen Energy

Citation (APA)
Bleeker, J., van Kasteren, C., van Ommen, J. R., & Vermaas, D. A. (2024). Gas bubble removal from a zero-gap alkaline electrolyser with a pressure swing and why foam electrodes might not be suitable at high current densities. *International Journal of Hydrogen Energy*, *57*, 1398-1407. https://doi.org/10.1016/j.ijhydene.2024.01.147

International Journal of Hydrogen Energy 57 (2024) 1398–1407

Contents lists available at ScienceDirect

International Journal of Hydrogen Energy

journal homepage: www.elsevier.com/locate/he

Gas bubble removal from a zero-gap alkaline electrolyser with a pressure swing and why foam electrodes might not be suitable at high current densities

Jorrit Bleeker, Celine van Kasteren, J. Ruud van Ommen, David A. Vermaas *

Department of Chemical Engineering, Delft University of Technology, 2629 HZ, Delft, Netherlands

ARTICLE INFO

Handling Editor: Ramazan Solmaz

Keywords:
Alkaline water electrolysis
Gas bubbles
Hydrogen
Zero-gap
Pressurized

ABSTRACT

To make green hydrogen more economically attractive, the energy losses in alkaline electrolysis need to be minimized while operating at high current densities (1 A cm^{-2}). At these current densities the ohmic resistance and gas bubbles effects contribute largely to the energy losses. To mitigate the gas bubbles losses, we demonstrate, for the first time, a pressure swing to remove gas bubbles in a zero-gap alkaline water electrolyzer. The pressure swing leverages the ideal gas law to increase the volume of gas in the system periodically, for a short duration (<2 s). This temporal volume increase effectively removes bubbles from the electrolyzer. We show that pressure swing can be used to measure the effect of bubbles on the ohmic resistance ($R_{Bubbles}$). Our results reveal that foam electrodes have a significantly larger $R_{Bubbles}$ than perforated plate electrodes (1.8 Ω cm^2 vs 0.3 Ω cm^2). The time-averaged cell voltage reduces by 170 mV when applying pressure swings to an electrolyzer operating at 200 mA cm^{-2} in 1 M KOH with foam electrodes. The bubble resistance further depends on the electrolyte conductivity (inversely proportional) and is only moderately affected by operating pressure (25 % lower when increasing pressure amplitude from 1–2 to 1–5 bar). By implementing these findings in a model, we estimate that the pressure swing could reduce the cell voltage by ~0.1 V for an electrolyzer operating at industrial conditions (6 M KOH, 80 °C, 1 A cm^{-2}) for foam electrodes. For perforated plate electrodes, however, the reduced cell voltage is lower and does not outweigh the additional compression energy.

1. Introduction

To limit global warming, fossil fuels need to be phased out as our main source of energy and chemicals [1,2]. Green hydrogen is indispensable for the fossil-free production of fertilizers, steel and chemicals [3]. IEA estimates that we will need 80 Mton of green hydrogen production by 2030 to be on track to net zero CO_2 emissions by 2050 [4], which is enormous compared to the predicted installed 0.45 Mton capacity by the end of 2023 [5].

To produce such large amounts of green hydrogen, we can use alkaline electrolysis [6]. Alkaline electrolysis benefits from its scalability as it uses abundant metal catalysts like iron and nickel, which is mandatory if we consider the required scale of hydrogen production [6,7]. Unfortunately, alkaline electrolysis is not economically attractive yet. The US department of energy calculated that the costs need to be reduced by 80 % to reach their target of 1 dollar per 1 kg H_2 [8]. These large cost reductions can only be achieved when the energy efficiency of alkaline electrolysis improves significantly at high current densities (1 A cm^{-2}) [9].

At high current densities the contribution of energy losses shifts towards ohmic losses (which scale linearly with current) and losses due to gas bubbles (which scale linearly or even more than linearly) [10–12]. The latter originates from hydrogen and oxygen bubbles that block the active sites on the electrodes and reduce the conductivity of the electrolyte solution [13–15]. This causes large energy losses, as the bubbles can take up more than 50 % of the volume of the electrolyzer [16].

Ohmic losses can be mitigated to some extent by reducing the interelectrode distance. This is why nowadays a large fraction of alkaline electrolysers are designed with an (almost) zero-gap design [9]. This design requires porous electrodes to ensure water and gas transport remains possible. Electrode geometries are that are typically used are metal foams [17,18], expanded meshes [19] and perforated plates [16,20]. However, a zero-gap configuration still suffers from bubbles, since gas gets stuck in the electrode pores and reduces the electrochemically

* Corresponding author.
E-mail address: D.A.Vermaas@tudelft.nl (D.A. Vermaas).

https://doi.org/10.1016/j.ijhydene.2024.01.147
Received 25 October 2023; Received in revised form 22 December 2023; Accepted 13 January 2024
Available online 19 January 2024

active surface area [16,21]. Not only do gas bubbles increase the ohmic resistance, they can also mechanically damage catalyst surfaces [22] and fluctuations in the electrical potential due to bubbles can lead to gradual degradation of the catalyst layer [23,24]. Creative methods to avoid and remove gas bubble are therefore crucial to fully optimize alkaline electrolyzers.

Gas bubble-mitigation strategies can be divided into three main approaches: Reducing gas bubble effects at the electrode microstructure level, electrode geometry level and at the process level.

Electrodes can be optimized at the microscale by creating nano- and micro-structured electrodes [25] (such as nanoneedles [26] and striped-pattern superlattices [24]). The sharp interfaces reduce the adhesion forces of gas bubbles, which results in a much faster release and thus 2–100x reduction in gas bubble sizes [24,26]. Additionally, electrodes with small hydrophobic have been synthesized to locally induce nucleation and collect gas, to keep the remaining electrode area

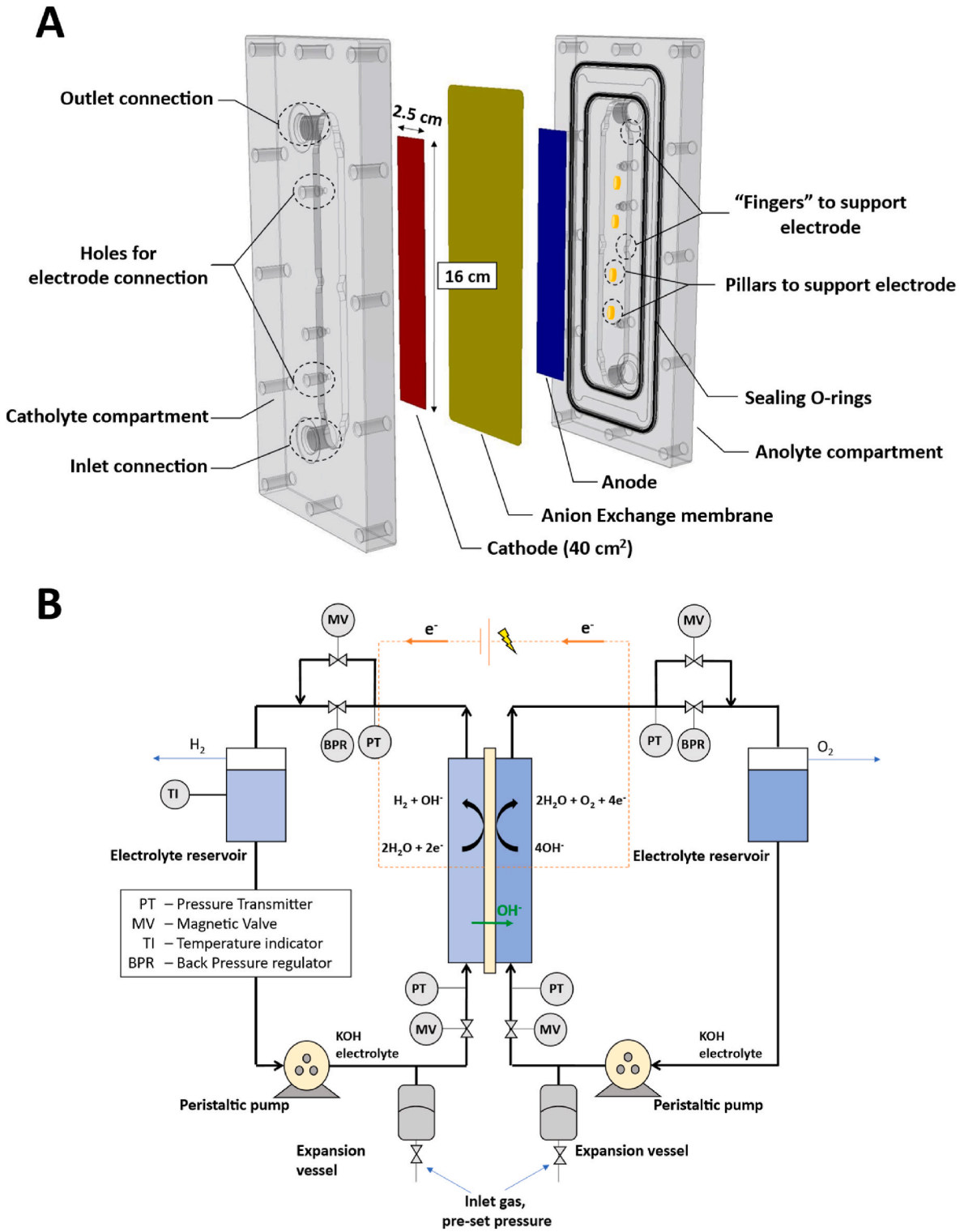

Fig. 1. **A.** Exploded diagram of the flow cell. **B.** Process diagram of the pressure swing setup, see SI-1 for the operation scheme of the pressure swing.

gas-free [27–29]. However, it is highly challenging to make such electrodes stable under high current densities at the hostile conditions of 30 wt% KOH and 80 °C for hundreds or even thousands of hours [30].

The macroscale electrode geometry can also mitigate the adverse effects of gas bubbles. The optimal geometry is a trade-off between a high electrochemically active surface area (ECSA) while keeping large enough pores to prevent bubble trapping in the pores. Previous work showed that mesh and foam electrodes with the highest ESCA can be outperformed by electrodes with a lower ECSA but large enough pores for bubble release [17,31,32]. Although, shape optimization and the use of non-standard electrode geometries [18,33,34] could result in even better gas-bubble mitigation, the complexity and trade-off with active surface area still limits the effectivity of this route for gas bubble mitigation.

On the process level the electrolyte, operating conditions and cell geometry can be optimized or on can apply external forces to reduce bubble effects. For example, Zhao et al. and others have shown that adding a surfactant to the electrolyte reduces the bubble nucleation energy and enhances bubble removal [22,35–37]. However, surfactants also cause foaming [26], which will make downstream gas-liquid separation more difficult. Operating the electrolyser at a higher pressure has minimal impact in zero-gap electrolysers; the stagnant bubbles ultimately release after reaching sufficient buoyancy, which means the bubble coverage is similar at low or high pressure in steady state [20,38] Gas bubble removal can be enhanced to some extent with turbulence promotors [39] or by having a “small-gap” instead of zero-gap [19]. Finally, gas bubbles can also actively be removed by process intensification, such as having an external force field [40–42], centrifugal flow [43], with ultrasound [44,45] or pressure waves [46]. Nevertheless, even with these strategies, gas bubble resistance remains a substantial part of the irreversible energy losses in electrolysis.

We introduce, for the first time, a pressure swing to remove gas bubbles in a zero-gap water electrolyzer. A pressure swing leverages the ideal gas law, by temporarily increasing the buoyancy and volume of gas bubbles at lower pressures. In our previous work [46], we showed that the average cell voltage can be reduced by 0.1–0.2 V applying a pressure swing (1–4 bar) periodically to an electrolyzer with a large gap. We have improved the response time of the pressure swing to be able to apply it to a zero-gap electrolyser. Here, we use the pressure swing to analyse and quantify the effect of gas bubbles on the cell voltage. We demonstrate that the cell voltage is reduced when applying a pressure swing to a zero-gap electrolyser, and that pressure swings can be leveraged to obtain in-operando information about the gas bubble coverage.

2. Method section

2.1. Electrochemical cell and materials

Pressure swing assisted electrolysis was performed in a custom-made rectangular Poly(methyl methacrylate) (PMMA) flow cell, see Fig. 1A. To achieve high transparency the PMMA was milled with a special diamond mill. The flow channels are 5 mm deep and 25 mm wide, and three polypropylene pillars (6 mm diameter) were added to keep the electrodes in place. The electrodes were either Ni Foam (Recemat BV, RCM-Ni4753.005, 0.5 mm thickness, 0.4 mm average pore diameter, 0.952 porosity) or Ni Perforated plate (Veco B.V., 0.3 mm thickness, 1.0 mm average pore size, 0.312 porosity). During experiments, the cathode and anode always had the same geometry (e.g. Foam/Foam). The electrodes have a geometric surface of 40 cm^2 and were pre-treated in situ. We welded two nickel wires to each electrode for electrical contact. The electrodes were separated by a Selemion AHO anion exchange membrane, which was used because of its good pressure-, gas-crossover- and alkalinity-resistance. EPDM O-rings (3 mm diameter, ERIKS) were used for sealing. The cell was pressure tested for 7 bar (abs).

2.2. Pressure swing equipment

The KOH catholyte and anolyte (45 wt% Thermo Scientific, diluted with demineralized water to 0.3, 1, 2, 3 or 6 M) are pumped through the system with peristaltic pumps at 72 mL/min (MasterFlex L/S with 16HP tubing, max pressure 8.5 bar). The maximum pressure in the electrolyser was controlled at the outlet with two back-pressure regulators (Swagelok, Stainless steel, Kalrez seals) to 2–5 bar (abs). The pressure swing was regulated with solenoid valves (Buschjost 82 560 series, Stainless steel) at the inlet (1/4″) and outlet (1/2”) of the electrolyser. To achieve a quick pressure response, membrane expansion vessels (Reflex Winkelmann GmbH, Reflex S2) were installed before the inlet solenoid valves. The gas cushion in the expansion vessels was pressurized with nitrogen to the desired operating pressure of the electrolyzer. See Fig. 1B for the process diagram of the system.

During high pressure operation, the inlet valve was open and the outlet solenoid was closed, and the liquid is exits the system through the back pressure regulator. The pressure swings were performed in four steps.

1. For 0.5 s, all valves are closed.
2. For 1 s, the outlet valve is opened. The system is now open to atmosphere and depressurizes. The pump continues pumping, but into the expansion vessel.
3. For 0.5 s, all valves are closed.
4. The inlet valve is opened again. High pressure liquid enters the system from the pump and expansion vessel.

This setup results in a pressure response of <1 s to achieve low pressure (step 2) and high pressure (step 4), which is much faster compared to previous work (5s to low pressure, ~20s to high pressure) [46].

The pressure was recorded with pressure transmitters (TC-Direct, 716–908) at the in- and outlet of the electrolyser. The temperature was recorded by a thermocouples in the catholyte bottle and the cathode and anode compartments inside the electrolyser (TC-Direct), during all measurements the temperature was 23–30 °C.

2.3. Electrochemical measurements

All alkaline electrolysis experiments were performed at constant current to ensure a constant gas production rate. The current was controlled with an Ivium XP20 Potentiostat. This was connected to the anode and cathode in a 4-electrode configuration to minimize ohmic losses in the voltage signal. Before every measurement series, the cell was operated at 200 mA cm^{-2} for 30 min at atmospheric pressure without a pressure swing. This was both to pretreat the electrodes and saturate the electrolytes with oxygen and hydrogen, to minimize Nernstian effects on the voltage.

In all $\Delta E_{Bubbles}$ measurements, the experiments were performed from high to low current densities, to minimize the effects of Ni redox reactions and effects from changes in dissolved gas concentration at lower currents.

2.4. Control and data acquisition

The pressure transmitters and thermocouples were read out with a NI-9207 and NI-9213 modules respectively and the solenoid valves were controlled with a NI-9482 relay module. The setup was controlled with a custom Labview script and the data was processed with in Python. All scripts are available on the Zenodo repository.

3. Results and discussion

We developed a pressure swing to remove hydrogen and oxygen gas bubbles from a zero-gap alkaline water electrolyser. First, the concept of

the pressure swing will be demonstrated and used to quantify the effects of gas bubbles on our zero-gap electrolyzer setup. Then pressure swing assisted electrolysis will be evaluated experimentally and with a simple analytical model.

3.1. Pressure swing concept in a zero-gap electrolyzer

The gas production in a zero-gap alkaline electrolyser is largest near the electrode separator interface [16], as the ionic travel distance between cathode and anode is the shortest here. A zero-gap configuration always has some small gap between the electrode and the separator. This is because the electrodes are not perfectly flat or the cell is compressed inhomogeneously [16,19] (see Fig. 2). As there is no easy path to release into the bulk electrolyte, gas bubbles tend to accumulate in this gap and in the pores of the electrode. The pressure swing is a method to remove gas bubbles from these the electrodes pores in three stages (Fig. 2).

1. Default operation at constant current and high pressure. The electrode and cell are saturated with gas bubbles. The cell voltage is high and fluctuating from constant detachment and coalescence of hydrogen and oxygen bubbles [47].
2. The pressure is reduced to atmospheric pressure for 1 s. This causes gas bubbles to expand. Bubbles inside the pores of the electrode are expanded and pushed out into the bulk electrolyte. During the low pressure stage the cell voltage increases, as all gas bubbles expand and further reduce the active electrode area and electrolyte conductivity. During stage 2 the pump is not connected to the electrolyser and the flow is driven by expanding gas bubbles.
3. The electrolyzer reconnected to the pump and pressurized by an inflow of high pressure electrolyte, which recompresses the remaining gas in the system. This flush of electrolyte removes the remaining gas bubbles from the bulk electrolyte. As the electrolyzer continuously produces new hydrogen and oxygen, the system will eventually transition back to stage 1.

To conclude, the pressure swing is an effective method for removing gas bubbles from the electrode surface of a zero-gap alkaline electrolyser The effectiveness of the bubble removal can be seen in the images in Fig. 2, videos in the **SI** and in the voltage response, where most of the fluctuations have disappeared during stage 3. The combination of the pressure pulse and the large flowrate in step 3 is key for good gas bubble removal. Our preliminary experiments have shown that a large flowrate pulse alone is not able to remove all gas (see **SI-2**).

3.1.1. Determining the ohmic contributions of gas bubbles ($R_{Bubbles}$)

The pressure swing allows us to measure the cell voltage of a electrolyzer in-situ with and without gas bubbles. When comparing the voltage directly after the pressure swing to the steady state voltage, the effects of gas bubbles ($\Delta E_{Bubbles}$) can be quantified (Fig. 3A) at the operating pressure, i.e. 4 bar in Fig. 3A. We acknowledge that $\Delta E_{Bubbles}$ could be underestimated because most, but not all, gas bubbles are removed, especially at higher current densities. $\Delta E_{Bubbles}$ could also be overestimated as the large inflow of fresh electrolyte could affect the concentration overpotential or induce slight changes in temperature. Swiegers et al. stated in their review article that estimates of bubble overpotentials are rare [12]. Because gas bubbles influence both the local current density and ohmic resistance, it is hard to isolate their contribution from other unrelated contributions to the overpotential. We believe that fast pressure swings, applied to electrolyzers in operando, could be a reliable approach to investigate and isolate bubble overpotentials ($\Delta E_{Bubbles}$). By installing (micro-)reference electrodes one could even measure $\Delta E_{Bubbles}$ on cathode and anode individually.

Fig. 3B shows the relation between $\Delta E_{Bubbles}$ and the current density for a Ni Foam electrode, 1 M KOH and a 1–2 bar pressure swing. $\Delta E_{Bubbles}$ is almost linear with current density until 150 mA cm^{-2}, with an $R_{Bubbles}$ slope of 1.8 Ω cm^2. The linearity indicates that gas bubbles in a zero-gap Ni Foam electrode cause an ohmic resistance, that is independent of the current up to 150 mA cm^{-2}. In other words, the rate of gas bubble production in the system does not seem to have a large effect on the bubble resistance. We believe this is caused by a saturated film of gas bubbles that forms in the electrode pores and in the electrode-separator gap, as was also suggested by others [16,21]. In Fig. 3B a lower $\Delta E_{Bubbles}$ slope is observed at >150 mA cm^{-2}. We believe this slope change is a results from the large gas production during the low pressure of the pressure swing. During the low pressure time at 150 mA cm^{-2}, 0.029 mL of H_2 gas is formed, which is 60 % of the pore volume of the foam. These remaining gas bubbles increase the voltage after a pressure swing, hence $\Delta E_{Bubbles}$ is no longer a true representation of the voltage change due to gas bubbles. These points were therefore not included in the $R_{Bubbles}$ slope fit.

After the pressure swing, the system will return to a steady state where the electrode pores are saturated with gas bubbles. We calculated this saturation timescale, t_{sat}, with a linear fit of the cell voltage (Fig. 3C). Here $t_{sat} = \Delta E_{Bubbles}/(dE/dt)_{fit}$. t_{sat} is inversely proportional to the current density (j) (Fig. 3D). We can further hypothesize that t_{sat} equals the bubble volume in the porous electrode at saturated conditions (V_0, in mL/cm^2) divided by the volumetric gas production rate:

$$t_{sat} = \frac{V_0}{j \frac{RT}{p\, n_{O2}\, F}} \quad \text{Eq 1}$$

in which j is the current density (mA cm^{-2}), R the ideal gas constant

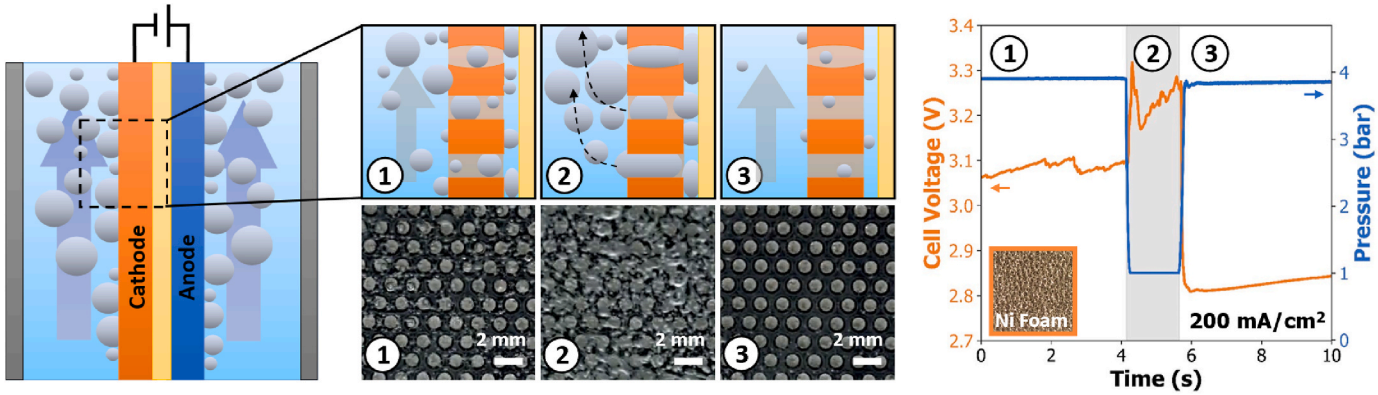

Fig. 2. Left/Middle top. Graphical representation bubble removal of a pressure swing in a zero gap alkaline water electrolyzer. Step 1. High pressure operation, Step 2 Low pressure step of the pressure swing, Step 3 Compression back to high pressure. **Middle bottom.** Images of oxygen bubbles on a Ni Perforated Plate anode during the pressure swing, 80 mA cm^{-2} **Right.** Voltage response to the pressure swing between 1 and 4 bar (abs), at 200 mA cm^{-2}, 1 M KOH, Ni Foam electrodes. The SI contains videos of the electrodes during a pressure swing.

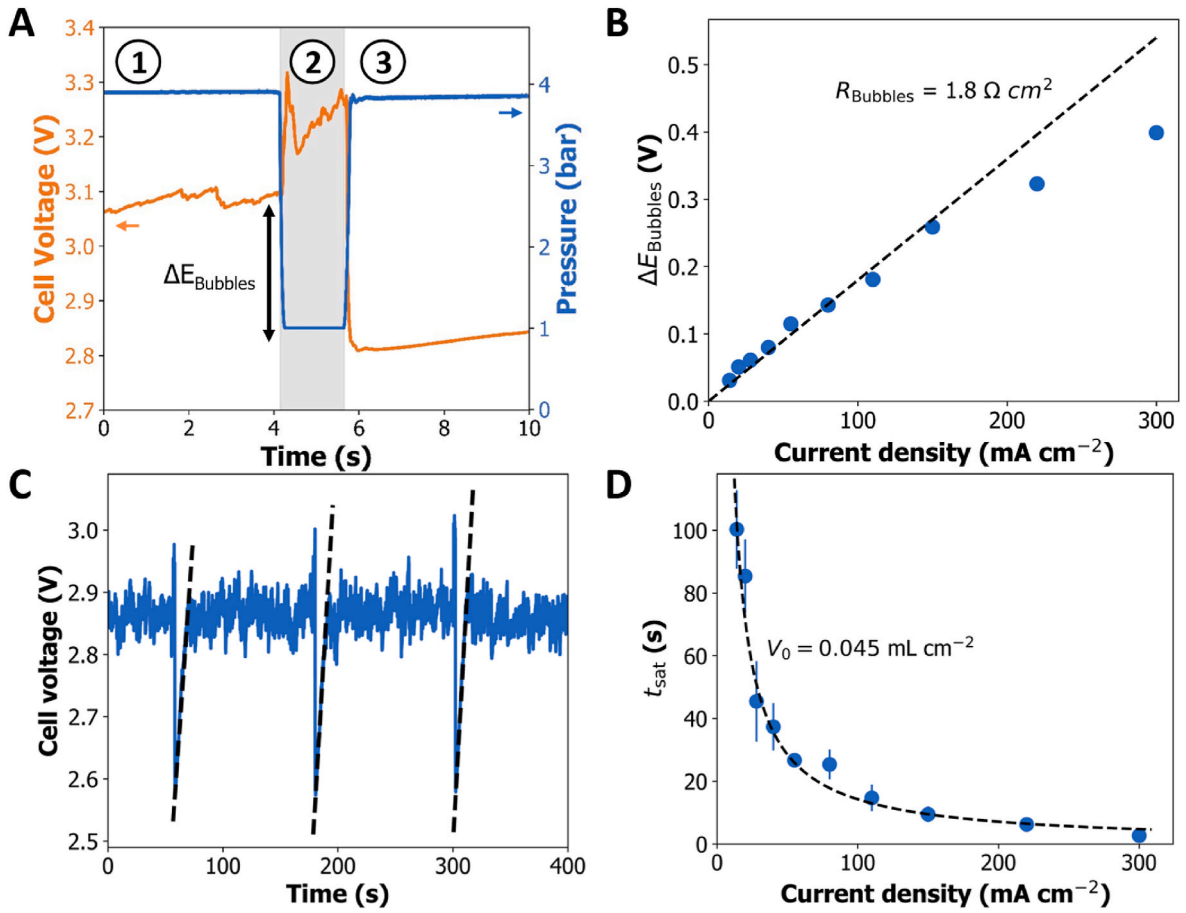

Fig. 3. A. Cell voltage drop after bubble removal with a pressure swing($\Delta E_{Bubbles}$) **B.** $\Delta E_{Bubbles}$ for various current densities, 1 M KOH, 1–2 bar pressure swing, Ni Foam. Linear fit until 150 mA cm^{-2} of $\Delta E_{Bubbles}$ results in a $R_{Bubbles}$ ($=\Delta E_{Bubbles}/j$) of 1.8 Ω cm^2 **C.** Cell voltage vs time for a 1–2 bar pressure swing, 150 mA cm^{-2}, 1 M KOH, Ni Foam. Linear fits were performed after pressure swing to find the dE_{cell}/dt. **D.** Saturation time after a 1–2 bar pressure swing, 1 M KOH, Ni Foam electrodes. Averaged over at least 10 pressure swings. Fitted with Eq (1) with a V_0 of 0.045 mL/cm^2.

(83.14 mL bar K^{-1} mol^{-1}), T temperature (K), p the pressure (bar), n_{O2} is 4 the ratio of electrons to oxygen and F the Faraday constant (9.6485 10^7 mC/mol). A least squares fit of the experimental data with Eq (1) resulted in a saturated gas volume V_0 of 0.045 mL/cm^2, which is similar to the specified pore volume of our Ni foam (0.048 mL/cm^2, **SI-3**). In steady operation, we therefore believe that most of the pores in the foam are filled with gas, independent of the current density.

3.1.2. *Effect of conductivity and pressure*

To further investigate $R_{Bubbles}$ we operated the pressure swing at different electrolyte concentrations and operating pressures. We expect $\Delta E_{Bubbles}$ to scale linearly with conductivity, if $R_{Bubbles}$ is ohmic in nature.

Fig. 4A shows $\Delta E_{Bubbles}$ for a 1–2 bar pressure swing at different concentrations of KOH. All concentrations show a linear relationship with current density. $R_{Bubbles}$ was calculated with a linear fit and scales inversely with electrolyte conductivity (Fig. 4B and **SI-4**), which further suggests that the effect of gas bubbles is mainly ohmic. Only at 0.3 M KOH other phenomena start to affect the ΔE after a pressure swing, such as temperature difference from ohmic heating and the concentration overpotential [19]. At 6 M KOH, $R_{Bubbles}$ is significantly lower than in an electrolyser with a 10 mm gap [46] but still substantial: 0.63 Ω cm^2 for a zero-gap system (this work) vs 0.91 Ω cm^2 for a gap system (Bakker et al., 2019, **SI-5**) [46]. This shows that a zero-gap with foam electrodes only reduces a fraction of the ohmic effects of gas bubbles.

The effect of operating pressure on $\Delta E_{Bubbles}$ was determined by changing the high pressure of the pressure swing (2, 3, 4 or 5 bar), while the low pressure was kept at atmospheric (Fig. 4C). We expect the operating pressure having only a small effect on $R_{Bubbles}$ at pressure swing timescales above t_{sat}. However, the effectivity of gas bubble removal is improved by the larger pressure difference. We observe that $\Delta E_{Bubbles}$ and $R_{Bubbles}$ only change by ~25 % at a 1–5 bar pressure swing compared to an electrolyser operating at 1–2 bar (see **SI-4** for $R_{Bubbles}$ values), while the pressure and gas bubble formation are 2.5 times higher. This is in agreement with the small effect of current density on $R_{Bubbles}$, which shows that the bubble resistance of a flow-by zero-gap electrolyzer is almost independent of the gas production rate. This was also observed in Fig. 3B and in literature [20,38,48].

The saturation time, t_{sat}, also follows **Eq (1)** at higher pressures (Fig. 4D). Also at higher pressures, the fitted volume V_0 is the same order of magnitude as the pore volume of the electrode. This indicates that the trapped gas volume inside the pores of the foam is independent of pressure. Bubble release at the electrode is therefore key, even for zero-gap configurations. To that end, other electrode geometries than foams, such as electrodes with a larger pore size, could result in a smaller $R_{Bubbles}$.

3.1.3. *Effect of electrode geometry*

Fig. 5A compares $\Delta E_{Bubbles}$ for a 1–2 bar pressure swing in 1 M KOH between foam and perforated plate electrodes. $R_{Bubbles}$ is calculated to be 1.8 Ω cm^2 and 0.3 Ω cm^2, for foam and perforated plate electrodes respectively. By just changing the electrodes, a 6 times reduction in $R_{Bubbles}$ can be achieved. This highlights the importance of selecting a suitable electrode geometry for mitigating gas bubble effects. Fig. 5B

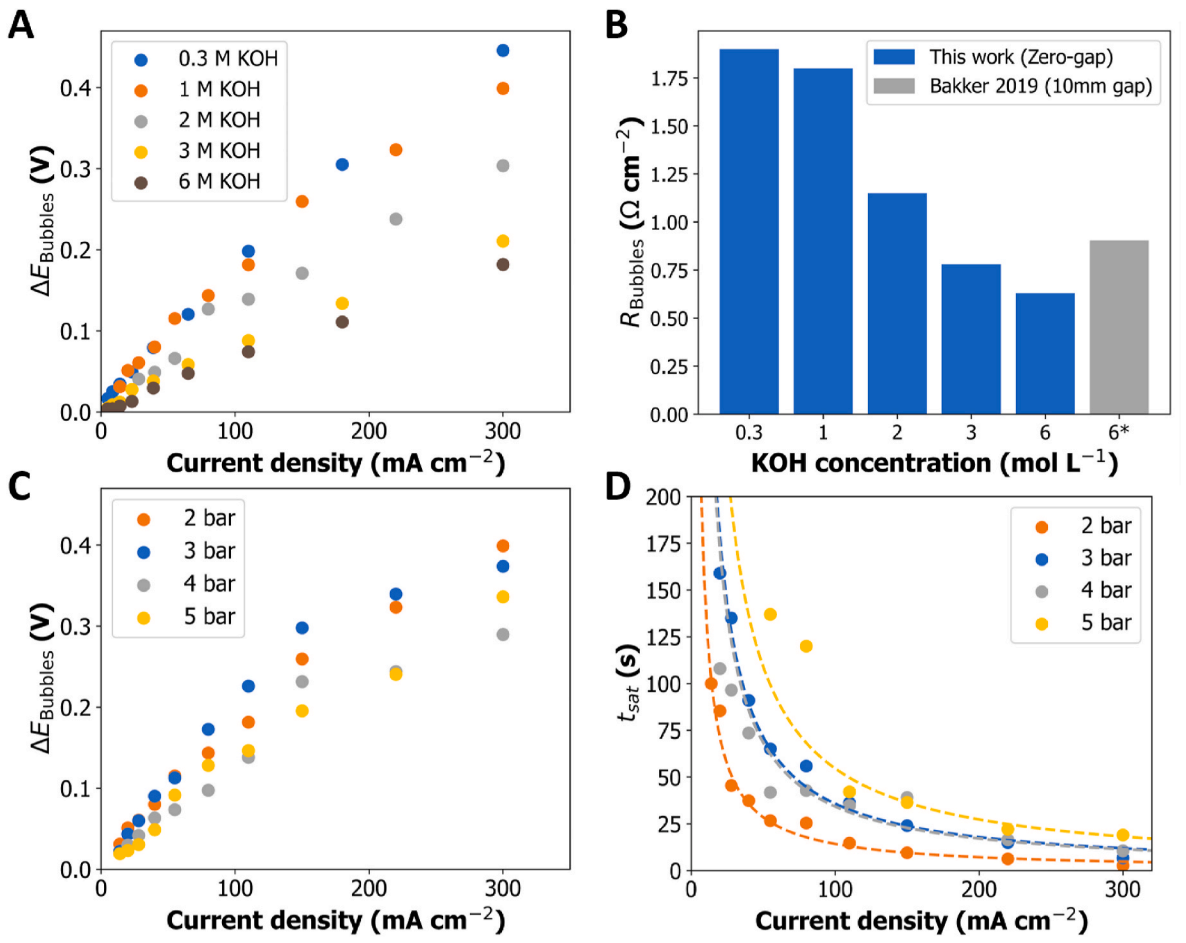

Fig. 4. Bubble effects on Ni Foam electrodes at different concentrations and pressures **A.** $\Delta E_{Bubbles}$ for a 1–2 bar pressure swing at different current densities and KOH concentrations, a linear fit was made to calculate the bubble resistance ($R_{Bubbles}$). **B.** Effect of KOH concentration on $R_{Bubbles}$. The 6 M KOH case is compared with a 10 mm gap electrolyser reported by Bakker and Vermaas [46] **C.** $\Delta E_{Bubbles}$ for 1–2, 1–3, 1–4 and 1–5 bar pressure swings in 1 M KOH **D.** Saturation time (t_{sat}) for the datapoints in C. Fitted with equation **Eq 1**. See **SI-4** for all fitted V_0 and $R_{Bubbles}$.

and **C** shows the voltage response over time to a pressure wing at 150 mA/cm^2 for the foam and perforated plate electrodes, respectively. After gas bubble removal, the voltage cell voltage for both electrodes is very similar (2.55–2.6 V). While the foam electrode has a linear increase in the voltage, the perforated plate seems to have a bi-modal pattern. First a quick increase in the voltage, followed by a slower buildup of voltage. Based on the timescales and the high speed videos in the **SI**, we believe this is because the electrode membrane gap is quickly filled with gas, after which the 1 mm pores of the perforated plate are filled more slowly. The larger timescale is because H_2 and O_2 bubbles, which have a typical diameter of 50–200 μm [49], can easily escape from the 1 mm pores. This confirms that high surface area electrodes do not always perform best and gas bubble management is equally important.

The $R_{Bubbles}$ of 0.3 Ω cm^2 measured for a 1 mm Ni Perforated plate electrode with the pressure swing, is of the same order of magnitude as simulations by de Groot and Vreman [16]. In addition to this, data from Kraglund shows that foam electrodes can have 4.7x higher $R_{Bubbles}$ than perforated plate electrodes [48] (for the comparison with literature, see **SI-5**). Although the geometries of his electrodes are different, the order of magnitude increase of $R_{Bubbles}$ is similar in our work. This demonstrates that the pressure swing is a suitable method to estimate bubble effects.

3.2. Reducing the cell voltage by applying pressure swings

We can leverage the pressure swing to reduce the average cell voltage of a zero-gap electrolyser by removing gas bubbles periodically. Two parameters can be varied to optimize the effects of a pressure swing: the high pressure time (t_{HP}) and the operating pressure. t_{HP} is the time the electrolyser operates at a high pressure between two pressure swings (Fig. 6A and **B**). Each pressure swing is most effective when the electrodes are saturated with gas bubbles, when $t_{HP} \geq t_{sat}$. An electrolyser operating under smaller t_{HP} removes gas bubbles more often. Although such a frequent pressure swing can keep the total amount of gas to a minimum, a too high pressure swing frequency compromises the cell voltage. At low t_{HP} the electrolyser will also be more often in the low pressure stage (stage 2 in Fig. 3A), where gas bubbles are expanded and the ohmic resistance is higher. Moreover, a small t_{HP} also requires more energy for the more frequent compressions. Similarly, at a high operating pressure, less pressure swings are required (as t_{sat} increases), but the compression costs of a single swing will be higher (see **SI-7** for an estimation of the compression costs).

In a zero-gap electrolyser with Ni foam electrodes operating at 1 M KOH, 1–2 bar pressure swings and 200 mA/cm^2, the average cell voltage can be reduced by 170 mV when applying pressure swings with a t_{HP} of 5 s (**Fig. 6C**). This is a 10 % reduction of the energy losses. When the additional compression energy consumption of the pressure swing are included into the cell voltage, the average cell voltage is reduced by 120 mV.

t_{sat} is around 7 s at 200 mA/cm^2 and 2 bar (see Fig. 4D), the optimal pressure swing frequency (5s in **Fig. 6C**) is faster than the saturation time. This is, however, a trade-off between compression costs and

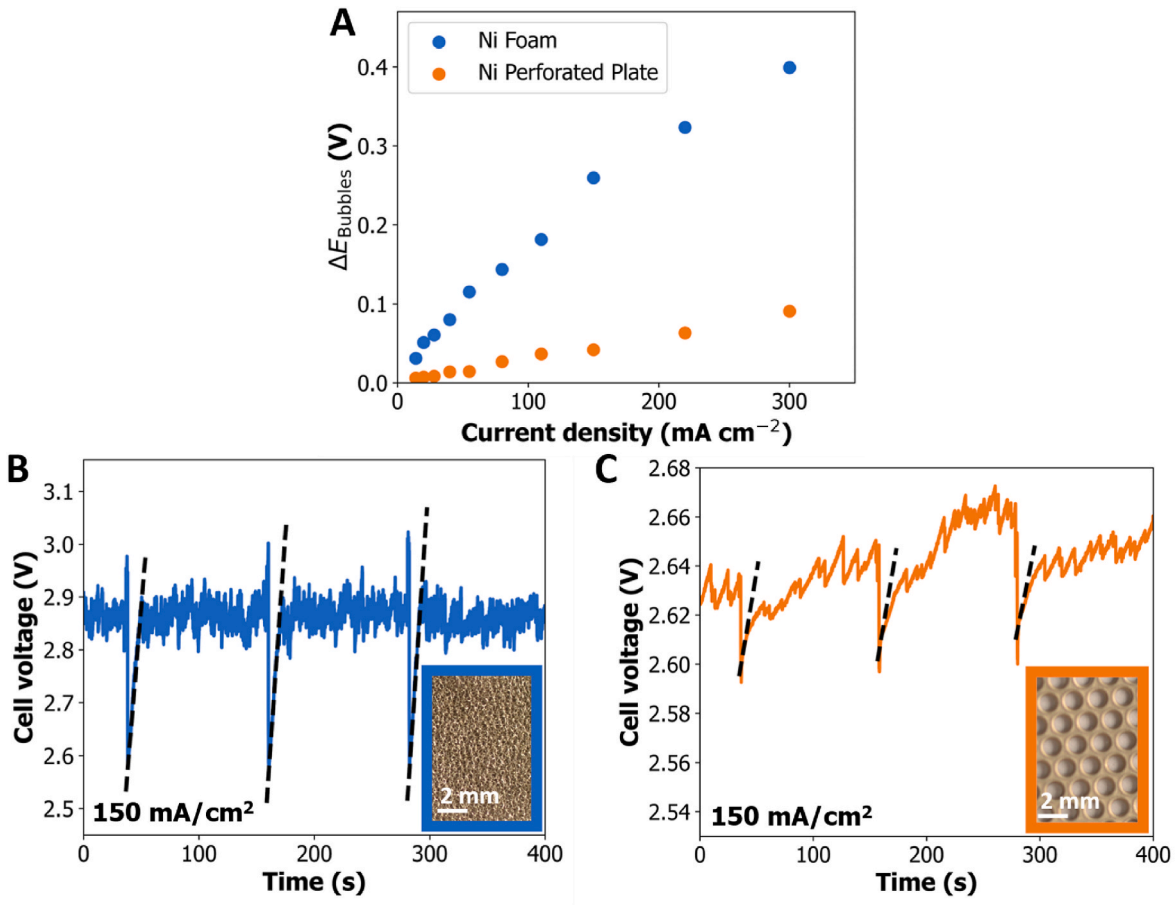

Fig. 5. A. Comparision of $\Delta E_{Bubbles}$ in Ni foam or perforated plate electrodes, 1–2 bar pressure swing and 1 M KOH **B.** Voltage/time response for an electrolyser with two Ni foam electrodes. Inset is a photo of the electrode. **C.** Voltage/time response for an electrolyser with two Ni perforated plate electrodes. See **SI-6** for larger photos of the electrode material.

voltage gain. We could not investigate at t_{HP} lower than 5 s, because our system did not pressurize in quick enough for the next pressure swing. In addition to this, at $t_{HP} < 5$ s pump energy quickly starts to become excessive and make the effects of the pressure swing redundant.

3.2.1. *Effect of operating pressure*

Fig. 6C and **D** shows the average cell voltage vs t_{HP} when operating under a 1–2 or 1–4 bar pressure swing (see **SI-8** for 1–3 and 1–5 bar pressure swings). At all pressures, the improvement of the average cell voltage was around 150 mV. Noticeable, at higher pressure the same improvement can be achieved at higher t_{HP}, which is a logical consequence of slower gas bubble saturation at higher applied pressure (Fig. 4D). However, the compression costs also increase with the higher pressure, also when taking into account the larger possible t_{HP}. When compression costs are included, the best performing pressure swing is between 1 and 2 bar, with an improvement of −120 mV in cell voltage.

Similar results are obtained at lower current densities (**SI-9**). Here, less gas is produced, so higher t_{HP} values still result in an improvement of the cell voltage. However the compression costs have a relatively bigger impact, as the power consumption of the electrolyser goes down, while the compression costs remain unchanged.

Although the pressure swing is effective at 1–2 bar and 200 mA/cm^2, higher current densities would require even smaller (<5 s) t_{HP} values, which can cause difficulties from an engineering point of view and would increase the compression costs. Increasing the low pressure and high pressure could be a solution for both problems. At high pressures higher t_{HP} values are possible and the compression costs scale with gas volume difference, so increasing the low pressure could make the pressure swing economically more attractive. For example, operating a hypothetical pressure swing between 30 and 40 bar could create a large average voltage improvement, while also saving on downstream hydrogen compression (compared to a system with a low pressure of 1 bar).

3.2.2. *Model analysis of pressure swing assisted electrolysis*

To assess the possibilities of pressure swing assisted alkaline electrolysis system, we calculated the change of the average cell voltage under various conditions. A simple analytical model was made (see **SI-11**) and implemented in Python. The compression costs of the pressure swing are included in these calculations. The model uses experimental values of this article (e.g. $R_{Bubbles}$ and V_0).

Fig. 7A predicts of how much the operating voltage of an electrolyzer can be improved by a 1–2 bar pressure swing. A room temperature electrolyzer (1 M KOH or 6 M KOH) with Nickel Foam electrodes could benefit significantly (<-0.2 V) from a pressure swing. However, an electrolyzer operating at industrial conditions (6 M KOH and 80 °C) will see limited, (0–0.1 V), improvements from a pressure swing. The red regions in Fig. 7 (>0 V) indicate operating regions where the compression energy costs outweigh the gain in operating voltage costs. The pressure swing should not be implemented in such a scenario. Fig. 7B shows that an electrolyzer with perforated plate electrodes will benefit little from a pressure swing. This is in agreement with our experiments, in which the effectiveness of a pressure swing in an electrolyser with perforated plates is limited (Fig. 5 and **SI-12**).

The reduction of the cell voltage is similar to other gas bubble techniques, like ultrasound [44] or supergravity [40], even after the

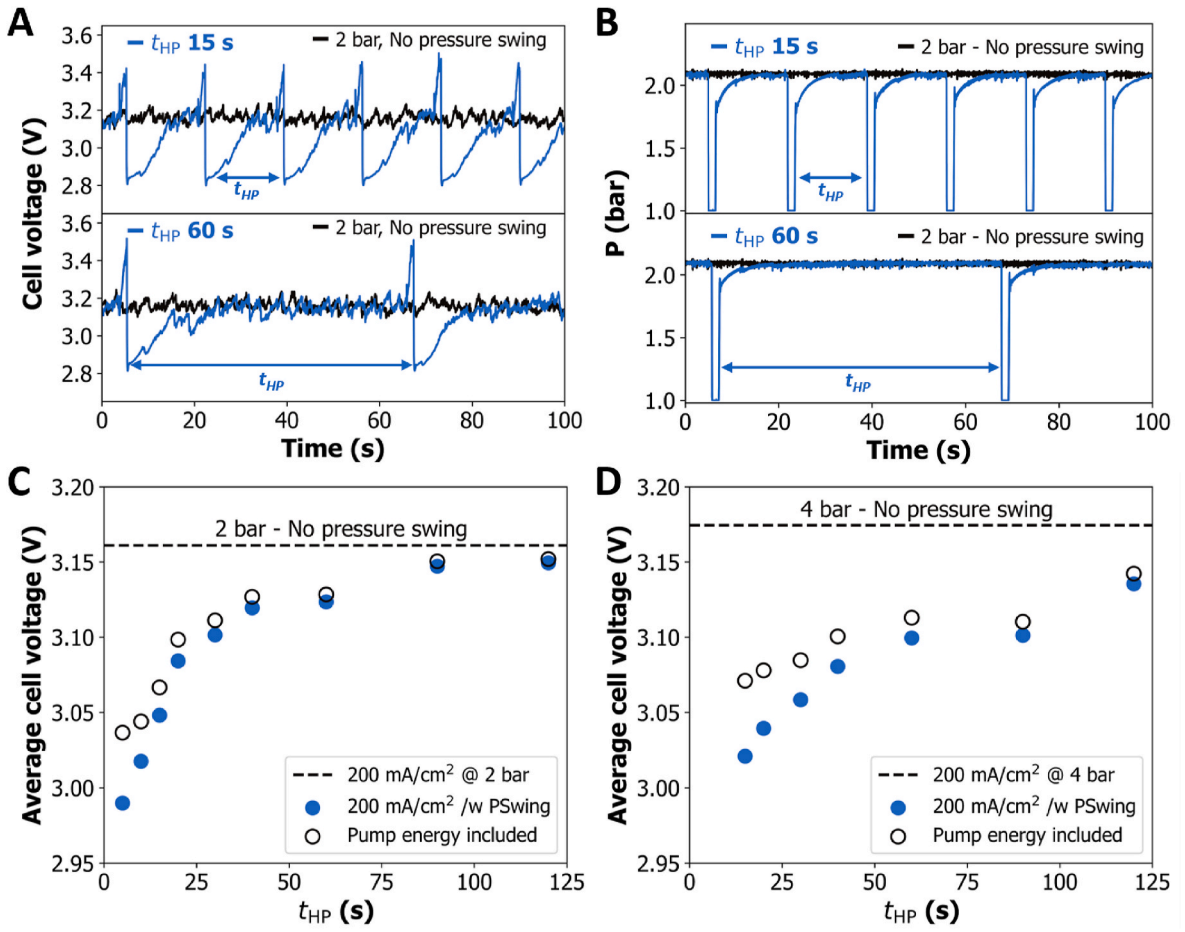

Fig. 6. 1 M KOH, Ni Foam electrodes **A**. Voltage response to a 1–2 bar pressure swing for two different high pressure times (t_{HP}). **B.** Pressure/time response of A. **C.** Average cell voltage for 1–2 bar pressure swings for different t_{HP}, compared to if no pressure swing was applied **D**. Average cell voltage for 1–4 bar pressure swings. Note: The cell voltage of 3.0–3.2 V is relatively high compared to similar systems in the literature [16,19,50]. We attribute this is to the high ohmic resistance of the Selemion AHO anion exchange membrane, which was used because of its high pressure resistance (12 bar), and the low electrolyte conductivity (1 M KOH @ 25–30 °C).

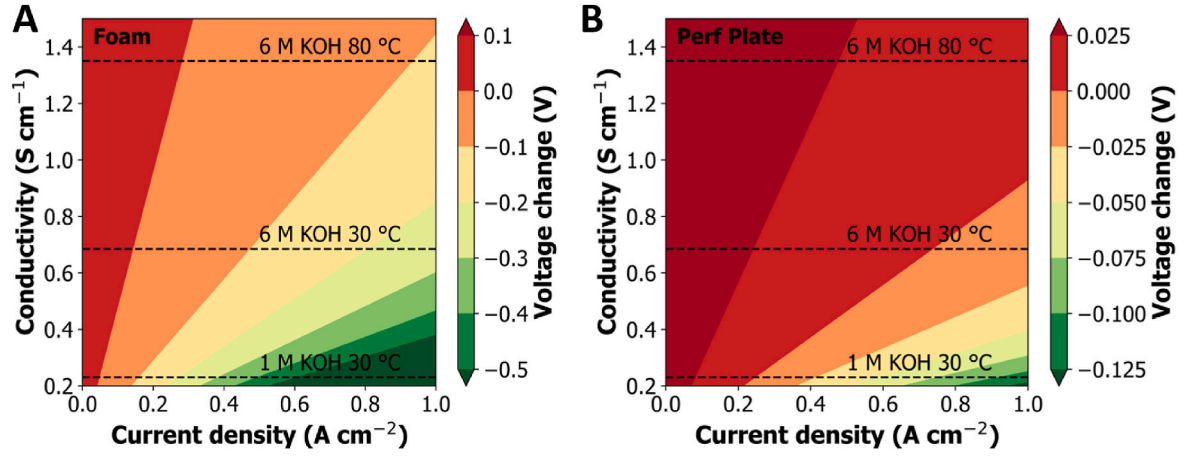

Fig. 7. Predicted maximum voltage change for a 1–2 bar pressure swing assisted zero-gap alkaline electrolyser as a function of current density and electrolyte conductivity. Compression costs of the pressure swing are included. See **SI-11** for the description of the model **A.** An electrolyzer operating with Ni foam electrodes **B.** Ni perforated plate electrodes.

additional energy costs for a pressure swing are taken into account. Additionally, a pressure swing can be implemented and scaled up relatively easily, as only an expansion tank and solenoid valves need to be installed at the in- and outlet of the electrolyzer. In comparison, ultrasound waves will dampen out and lose strength over larger electrolyser stacks and supergravity through centrifuges becomes more difficult to implement at large systems. Pressure swing-assisted electrolysis can also easily be combined with other bubble mitigation

strategies (i.e. superwetting electrodes or flow-through electrolysers) to minimize bubble effects.

However, the implementation of a pressure swing on an industrial alkaline electrolysis plant will also bring some difficulties. Large pressure differences, fast-moving valves and pumps increase the amount of hazards in a plant and will require extra maintenance and monitoring. In addition, the pressure swing will also results in a fluctuating voltage (or fluctuating current when operating at constant voltage), which is challenging to supply at a large scale and could damage catalyst surfaces.

While the application of a pressure swing on an industrial electrolyser might be difficult, it has promise as a testing rig to analyse the effects of gas bubbles in various electrolyser designs. Gas bubble removal with a pressure swing allows to decouple the effects of gas bubbles from the total ohmic resistance. Furthermore, the technique could also be used for gas bubble removal from porous materials in different systems, such as H_2 generation from borohydrides [51], fouling removal in membrane processes [52] or CO_2 capture with organic redox agents [53].

4. Conclusions

The effects of gas bubbles on the cell voltage in a zero-gap alkaline electrolyser were investigated with a pressure swing. We demonstrate a pressure swing which removes gas bubbles attached to the electrode in a fast (<1s) swing between high pressure (2–5 bar) and atmospheric pressure.

A zero-gap configuration still suffers from gas bubbles, represented by a substantial bubble resistance $R_{Bubbles}$, although the bubble effects are smaller than in a regular gap electrolyser. $R_{Bubbles}$ strongly depends on the electrode geometry; a Ni Perforated plate has a much lower bubble resistance (0.3 Ω cm^2, 1 M KOH 30 °C) than a Foam electrode (1.8 Ωcm^2, 1 M KOH 30 °C). By investigating the saturation time, it was discovered that the gas bubble volume ($V_0 = 0.045$ mL/cm^2) is close to the pore volume in foam electrodes (0.048 mL/cm^2), which means that foam electrodes in a flow-by configuration are almost completely filled with gas bubbles. The timescale for gas saturation is in the second (<5s) range at 2 bar, the optimal time between two pressure swings (t_{HP}) is around 5 s too. Finally, under industrial conditions (6 M KOH, 80 °C) a pressure swing could reduce the cell voltage by 0.1 V at 1 A/cm^2 for foam electrodes. However, this is mainly because foam electrodes have a very large bubble resistance. In perforated plate electrodes the energy gain of a pressure swing is limited because the required compression energy can be larger than the voltage gain by removing gas under industrial conditions. We believe that the pressure swing has therefore most value as a gas bubble analysis method at both scientific and industrial scale.

Data availability

The data supporting the findings of this study are contained within the paper and its associated Supplementary Information. All other relevant data is available from the corresponding author upon reasonable request and in the Zenodo repository at 10.5281/zenodo.7802110.

Author contributions

J.B. and C.K. designed and built the setup. J.B. performed experiments and analysed the data. D.V. and J.R.vO. supervised the project. D. V. acquired funding. J.B. wrote the paper. All the authors discussed and contributed to the writing.

Declaration of competing interest

The authors declare that they have no known competing financial interests or personal relationships that could have appeared to influence the work reported in this paper.

Acknowledgements

The authors thank Christiaan Schinkel, Duco Bosma, Evert Wagner, Kevin Kamman and Stefan ten Hagen (TU Delft) for their technical support and Willem Haverkort, Wouter van der Does (TU Delft), Thijs de Groot and Rodrigo Barros (TU Eindhoven) for the insightful discussions.

This project has received funding from the European Research Council (ERC) under the European Union's Horizon 2020 research and innovation programme (grant agreement No 852115). This work reflects the authors' view and the ERC Executive Agency is not responsible for any use resulting from the information it contains.

Appendix A. Supplementary data

Supplementary data to this article can be found online at https://doi.org/10.1016/j.ijhydene.2024.01.147.

References

[1] Pörtner H-O, Roberts DC, Adams H, Adler C, Aldunce P, Ali E, et al. Climate change 2022: impacts, adaptation and vulnerability. Switzerland: IPCC Geneva; 2022.
[2] New M, Liverman D, Schroder H, Anderson K. Four degrees and beyond: the potential for a global temperature increase of four degrees and its implications. Phil Trans Math Phys Eng Sci 2011;369:6–19.
[3] Capurso T, Stefanizzi M, Torresi M, Camporeale SM. Perspective of the role of hydrogen in the 21st century energy transition. Energy Convers Manag 2022;251:114898.
[4] IEA. Global hydrogen review. Paris: IEA; 2021. https://wwwieaorg/reports/global-hydrogen-review-2021. License: CC BY 40. 2021.
[5] IEA. Tracking electrolysers. IEA; 2023. https://wwwieaorg/energy-system/low-emission-fuels/electrolysers#tracking. License: CC BY 40.
[6] Brauns J, Turek T. Alkaline water electrolysis powered by renewable energy: a review. Processes 2020;8:248.
[7] Sapountzi FM, Gracia JM, Weststrate CJ, Fredriksson HOA, Niemantsverdriet JW. Electrocatalysts for the generation of hydrogen, oxygen and synthesis gas. Prog Energy Combust Sci 2017;58:1–35.
[8] US Department of Energy. Secretary granholm launches hydrogen energy earthshot to accelerate breakthroughs toward a net-zero economy. 2021.
[9] Krishnan S, Koning V, Theodorus de Groot M, de Groot A, Mendoza PG, Junginger M, et al. Present and future cost of alkaline and PEM electrolyser stacks. Int J Hydrogen Energy 2023;48:32313–30.
[10] Zeng K, Zhang D. Recent progress in alkaline water electrolysis for hydrogen production and applications. Prog Energy Combust Sci 2010;36:307–26.
[11] Phillips R, Dunnill Charles W. Zero gap alkaline electrolysis cell design for renewable energy storage as hydrogen gas. RSC Adv 2016;6:100643–51.
[12] Swiegers GF, Terrett RNL, Tsekouras G, Tsuzuki T, Pace RJ, Stranger R. The prospects of developing a highly energy-efficient water electrolyser by eliminating or mitigating bubble effects. Sustain Energy Fuels 2021;5:1280–310.
[13] Vogt H. The actual current density of gas-evolving electrodes—notes on the bubble coverage. Electrochim Acta 2012;78:183–7.
[14] Vogt H. The incremental ohmic resistance caused by bubbles adhering to an electrode. J Appl Electrochem 1983;13:87–8.
[15] Deng X, Yang F, Li Y, Dang J, Ouyang M. Quantitative study on gas evolution effects under large current density in zero-gap alkaline water electrolyzers. J Power Sources 2023;555:232378.
[16] de Groot MT, Vreman AW. Ohmic resistance in zero gap alkaline electrolysis with a Zirfon diaphragm. Electrochim Acta 2021;369:137684.
[17] Rocha F, Delmelle R, Georgiadis C, Proost J. Effect of pore size and electrolyte flow rate on the bubble removal efficiency of 3D pure Ni foam electrodes during alkaline water electrolysis. J Environ Chem Eng 2022;10:107648.
[18] Rocha F, Delmelle R, Georgiadis C, Proost J. Electrochemical performance enhancement of 3D printed electrodes tailored for enhanced gas evacuation during alkaline water electrolysis. Adv Energy Mater 2023;13:2203087.
[19] Haverkort JW, Rajaei H. Voltage losses in zero-gap alkaline water electrolysis. J Power Sources 2021;497:229864.
[20] de Groot MT, Kraakman J, Garcia Barros RL. Optimal operating parameters for advanced alkaline water electrolysis. Int J Hydrogen Energy 2022;47:34773–83.
[21] Kienzlen V, Haaf D, Schnurnberger W. Location of hydrogen gas evolution on perforated plate electrodes in zero gap cells. Int J Hydrogen Energy 1994;19:729–32.
[22] Zhao X, Ren H, Luo L. Gas bubbles in electrochemical gas evolution reactions. Langmuir 2019;35:5392–408.
[23] Lee JK, Bazylak A. Bubbles: the good, the bad, and the ugly. Joule 2021;5:19–21.
[24] Song Q, Xue Z, Liu C, Qiao X, Liu L, Huang C, et al. General strategy to optimize gas evolution reaction via assembled striped-pattern superlattices. J Am Chem Soc 2020;142:1857–63.
[25] Brinkert K, Richter MH, Akay Ö, Liedtke J, Giersig M, Fountaine KT, et al. Efficient solar hydrogen generation in microgravity environment. Nat Commun 2018;9:2527.

[26] Burdyny T, Graham PJ, Pang Y, Dinh C-T, Liu M, Sargent EH, et al. Nanomorphology-enhanced gas-evolution intensifies CO2 reduction electrochemistry. ACS Sustainable Chem Eng 2017;5:4031–40.
[27] Brussieux C, Viers P, Roustan H, Rakib M. Controlled electrochemical gas bubble release from electrodes entirely and partially covered with hydrophobic materials. Electrochim Acta 2011;56:7194–201.
[28] Heidrich HJ, Müller L. The effect of hydrophobic centres on the electrode surface on overvoltage in electrochemical gas evolution. Electrochim Acta 1990;35:1089–93.
[29] Kadyk T, Bruce D, Eikerling M. How to enhance gas removal from porous electrodes? Sci Rep 2016;6:38780.
[30] Todoroki N, Wadayama T. Electrochemical stability of stainless-steel-made anode for alkaline water electrolysis: surface catalyst nanostructures and oxygen evolution overpotentials under applying potential cycle loading. Electrochem Commun 2021;122:106902.
[31] Li L, Jiang W, Zhang G, Feng D, Zhang C, Yao W, et al. Efficient mesh interface engineering: insights from bubble dynamics in electrocatalysis. ACS Appl Mater Interfaces 2021;13:45346–54.
[32] Lee HI, Cho H-S, Kim M, Lee JH, Lee C, Lee S, et al. The structural effect of electrode mesh on hydrogen evolution reaction performance for alkaline water electrolysis. Front Chem 2021;9.
[33] Yang F, Kim MJ, Brown M, Wiley BJ. Alkaline water electrolysis at 25 A cm−2 with a microfibrous flow-through electrode. Adv Energy Mater 2020;10:2001174.
[34] Kou T, Wang S, Shi R, Zhang T, Chiovoloni S, Lu JQ, et al. Periodic porous 3D electrodes mitigate gas bubble traffic during alkaline water electrolysis at high current densities. Adv Energy Mater 2020;10:2002955.
[35] Zhao X, Ranaweera R, Luo L. Highly efficient hydrogen evolution of platinum via tuning the interfacial dissolved-gas concentration. Chem Commun 2019;55:1378–81.
[36] Xie Q, Zhou D, Li P, Cai Z, Xie T, Gao T, et al. Enhancing oxygen evolution reaction by cationic surfactants. Nano Res 2019;12:2302–6.
[37] Hosseini SR, Ghasemi S, Ghasemi SA. Effect of surfactants on electrocatalytic performance of copper nanoparticles for hydrogen evolution reaction. J Mol Liq 2016;222:1068–75.
[38] Jang D, Cho H-S, Kang S. Numerical modeling and analysis of the effect of pressure on the performance of an alkaline water electrolysis system. Appl Energy 2021;287:116554.
[39] Weusten SJC, Murrer LCEM, de Groot MT, van der Schaaf J. Mass transfer in 3D-printed electrolyzers: the importance of inlet effects. AIChE J 2021;67:e17263.
[40] Cheng H, Scott K, Ramshaw C. Intensification of water electrolysis in a centrifugal field. J Electrochem Soc 2002;149:D172.
[41] Sakuma G, Fukunaka Y, Matsushima H. Nucleation and growth of electrolytic gas bubbles under microgravity. Int J Hydrogen Energy 2014;39:7638–45.
[42] Iida T, Matsushima H, Fukunaka Y. Water electrolysis under a magnetic field. J Electrochem Soc 2007;154:E112.
[43] Chen Z, Meng C, Ruan H, Li R, Xu X, Liu B, et al. Removal of bubbles from eletrodes in a planar cyclonic electrolyzer. Chem. Eng. Process. Intensif. 2022;181:109133.
[44] Li S-D, Wang C-C, Chen C-Y. Water electrolysis in the presence of an ultrasonic field. Electrochim Acta 2009;54:3877–83.
[45] McMurray H N. Hydrogen evolution and oxygen reduction at a titanium sonotrode. Chem Commun 1998:887–8.
[46] Bakker MM, Vermaas DA. Gas bubble removal in alkaline water electrolysis with utilization of pressure swings. Electrochim Acta 2019;319:148–57.
[47] Hodges A, Hoang AL, Tsekouras G, Wagner K, Lee C-Y, Swiegers GF, et al. A high-performance capillary-fed electrolysis cell promises more cost-competitive renewable hydrogen. Nat Commun 2022;13:1304.
[48] Kraglund MR. Alkaline membrane water electrolysis with non-noble catalysts. 2017.
[49] Janssen L, Sillen C, Barendrecht E, Van Stralen S. Bubble behaviour during oxygen and hydrogen evolution at transparent electrodes in KOH solution. Electrochim Acta 1984;29:633–42.
[50] Kraglund MR, Carmo M, Schiller G, Ansar SA, Aili D, Christensen E, et al. Ion-solvating membranes as a new approach towards high rate alkaline electrolyzers. Energy Environ Sci 2019;12:3313–8.
[51] Liang Y, Wang P, Dai H-B. Hydrogen bubbles dynamic template preparation of a porous Fe–Co–B/Ni foam catalyst for hydrogen generation from hydrolysis of alkaline sodium borohydride solution. J Alloys Compd 2010;491:359–65.
[52] Sharifian R, van der Wal HC, Wagterveld RM, Vermaas DA. Fouling management in oceanic carbon capture via in-situ electrochemical bipolar membrane electrodialysis. Chem Eng J 2023;458:141407.
[53] Diederichsen KM, Liu Y, Ozbek N, Seo H, Hatton TA. Toward solvent-free continuous-flow electrochemically mediated carbon capture with high-concentration liquid quinone chemistry. Joule 2022;6:221–39.